Т. 86, № 1 ЖУРНАЛ ПРИКЛАДНОЙ СПЕКТРОСКОПИИ ЯНВАРЬ — ФЕВРАЛЬ 2019
V. 86, N 1 JOURNAL OF APPLIED SPECTROSCOPY JANUARY — FEBRUARY 2019

ANALYSIS OF NITROPOLYCYCLIC AROMATIC HYDROCARBONS IN FINE PARTICULATE MATTER BY MATRIX-ASSISTED LASER DESORPTION/IONIZATION TIME-OF-FLIGHT MASS SPECTROMETRY USING Fe_3O_4/ZIF-8 MAGNETIC NANOCOMPOZITES AS MATRIX

Haojiang Wang [1], Xuan Wang [2], Wei Bian [1*], Tijian Sun [1*], Zongwei Cai [3], Jiancong Wei [1*]

[1] School of Basic Medical Science, Shanxi Medical University,
Taiyuan 030001, China; e-mail: sxykdx_bianwei@163.com
[2] College of Pharmacy, Shanxi Medical University, Taiyuan 030001, China
[3] Hong Kong Baptist University, State Key Laboratory of Environmental and Biological Analysis,
Hong Kong SAR, China

Core-shell magnetic metal organic nanocrystals were synthesized and used as matrix for matrix-assisted laser desorption/ionization time-of-flight mass spectrometry (MALDI-TOF MS). Four nitropolycyclic aromatic hydrocarbons (nitro-PAHs) were successfully detected by using negative-ion MALDI-TOF MS without background interference. Furthermore, the magnetic nanocomposites (MNCs) coated with zeolitic imidazolate framework-8 (ZIF-8) showed excellent adsorption and enrichment capacity, and can be isolated with a magnet and directly spotted on the stainless steel plate for MALDI measurement. It was also analyzed nitro-PAHs in PM2.5 samples using the ZIF-8-coated magnetic nanocomposite as adsorbent and matrix.

Keywords: *matrix-assisted laser desorption/ionization time-of-flight mass spectrometry, Fe_3O_4/ZIF-8 magnetic nanocomposites, nitropolycyclic aromatic hydrocarbons, enrichment and analysis.*

АНАЛИЗ НИТРОПОЛИЦИКЛИЧЕСКИХ АРОМАТИЧЕСКИХ УГЛЕВОДОРОДОВ В МЕЛКИХ ТВЕРДЫХ ЧАСТИЦАХ МЕТОДОМ ВРЕМЯПРОЛЕТНОЙ МАСС-СПЕКТРОМЕТРИИ НА ОСНОВЕ ЛАЗЕРНОЙ ДЕСОРБЦИИ/ИОНИЗАЦИИ С ИСПОЛЬЗОВАНИЕМ МАГНИТНЫХ НАНОКОМПОЗИТОВ Fe_3O_4/ZIF-8 В КАЧЕСТВЕ МАТРИЦЫ

H. Wang [1], X. Wang [2], W. Bian [1*], T. Sun [1*], Z. Cai [3], J. Wei [1*]

УДК 543.42;620.3

[1] Школа фундаментальной медицины, Медицинский университет Шаньси,
Тайюань 030001, Китай; e-mail: sxykdx_bianwei@163.com
[2] Фармацевтический колледж, Медицинский университет Шаньси, Тайюань 030001, Китай
[3] Баптистский университет Гонконга, Гонконг, Китай

(Поступила 21 августа 2017)

Синтезированные двуслойные магнитные металлорганические нанокристаллы использованы в качестве матрицы для времяпролетной масс-спектрометрии на основе лазерной десорбции/ионизации (MALDI-TOF MS). Четыре нитрополициклических ароматических углеводорода (нитро-ПАУ) успешно обнаружены методом MALDI-TOF MS с использованием отрицательных ионов без фоновых помех. Магнитные нанокомпозиты, покрытые цеолитовой имидазолатной оболочкой (ZIF-8), показали отличную адсорбционную и обогащающую способность и могут быть изолированы магнитом и непосредственно нанесены на пластину из нержавеющей стали для измерения методом MALDI. Проанализированы нитро-ПАУ в образцах PM2.5 с использованием покрытого оболочкой ZIF-8 магнитного нанокомпозита в качестве адсорбента и матрицы.

Ключевые слова: *времяпролетная масс-спектрометрия на основе лазерной десорбции/ионизации, Fe_3O_4/ZIF-8 магнитные нанокомпозиты, нитрополициклические ароматические углеводороды, обогащение и анализ.*

Introduction. In recent years, the widespread haze accompanied by high-PM2.5 pollution during winter in Chinese cities has attracted considerable attention [1]. Ambient PM2.5, a fine particulate matter with ≤2.5 μm aerodynamic diameter, mainly stems from coal combustion, vehicle exhausts, and other open sources, and could increase the risk of respiratory diseases and lung cancer [2–4]. PM2.5 toxicity is not only caused by the direct effect of particle size but also from adsorbed chemical substances, such as polycyclic aromatic hydrocarbons (PAHs), nitro-PAHs, and ions. Moreover, nitro-PAHs, which are apt to partition onto PM2.5 and increasingly accumulate in the aerosol phase, have been indicated as a class of potentially mutagenic and carcinogenic environmental pollutants [5, 6]. Therefore, considerable efforts are continuously spent to improve the simplicity, sensitivity, selectivity, and utility of methods for the determination of nitro-PAHs in $PM_{2.5}$ particles.

As MALDI-TOF MS possesses advantages of rapid analysis, simple pretreatment procedure, and low consumption of samples, this technology has been extensively applied to analyze proteins, other macromolecules [7], and microbes [8]. The application of MALDI-TOF MS in the analysis of small molecules has significant limitations due to the background interference of conventional organic matrices in the low mass region (<500 Da) and the poor reproducibility derived from the inhomogeneity of the matrix-analyte crystals [9]. Surface-assisted laser desorption/ionization mass spectrometry (SALDI-MS) has been developed to overcome these shortcomings by using nanomaterials as matrices [10]. In recent years, numerous nanomaterials with large surface areas, including carbon-based materials [11–14], metal nanoparticles [15, 16], and porous silicon [17, 18], have come to the fore as burgeoning matrixes for SALDI-MS [10, 19–21]. SALDI-MS had some success. Most developments are focused on the analysis of small molecules, such as amino acids, fatty acids, peptides, and drugs in biological field, but the reports on environmental pollutants in environmental samples such as PM2.5 are few. Thus, exploring a new matrix for detecting nitro-PAHs in PM2.5 using SALDI-MS is highly desirable.

The zeolitic imidazolate framework (ZIF) materials with their exceptional chemical and thermal stabilities have zeolite-like topologies and belong to an important class of metal-organic framework (MOF) materials, which have exciting adsorption, porosity, separation capability, and catalytic properties [22, 23]. 2-Methylimidazole (HMeIM), which is the main ingredient of ZIF-8, has the capacity to capture protons from analytes upon their desorption due to the possession sp^2-hybridized nitrogen [15]. Therefore, ZIF-8 is anticipated to produce affluent negative ions in negative-ion mode by speeding up the negative-charged process. In addition, magnetic nanoparticles, with unique magnetic separation ability, can simplify the isolation step and accelerate the assay process.

ZIF-8-coated magnetic nanocomposites (Fe_3O_4/ZIF-8 MNCs) can effectively increase the magnetic property of the MOF material and achieve its further effective application in sample pretreatment [24, 25]. Cai's group [21] analyzed small molecules, including amino acids, fatty acids, and hormones, using Fe_3O_4/ZIF-8 MNC as a matrix through negative-ion MALDI-TOF MS. No report is available on the research of detecting environmental pollutants in PM2.5 applying MALDI-TOF MS with Fe_3O_4/ZIF-8 MNC as the matrix.

Herein, Fe_3O_4/ZIF-8 MNCs were fabricated by a facile channel and used to detect four nitro-PAHs as alternative matrices in SALDI-MS assays instead of traditional organic compounds. We probed four nitro-PAHs (1-nitropyrene (1-NP), 2-nitrofluorene (2-NFL), 6-nitrochrysene (6-NC), and 9-nitroanthracene [9-NA]) as test analytes to estimate the potential of Fe_3O_4/ZIF-8 MNCs as matrices to detect environmental pollutants. The method was successfully used for the analysis of nitro-PAHs in PM2.5 samples.

Experimental. Ferric chloride hexahydrate ($FeCl_3 \cdot 6H_2O$), sodium acetate (NaAC), sodium citrate dehydrate ($Na_3Cit \cdot 2H_2O$), ethylene glycol, and $Zn(NO_3)_2 \cdot 6H_2O$ were obtained from Sinopharm Chemical Reagent, Co., Ltd (Shanghai, China). 3-(N-Morpholino)propanesulfonic acid (MOPS) and triuoroacetic acid were obtained from Aladdin Chemistry Co., Ltd (Shanghai, China). Standards of 1-NP, 6-NC, and 9-NA were obtained from Sigma (USA). 2-NFL was purchased from Accu standard, Inc. (USA). High-purity water was used from a Milli-Q-RO$_4$ water purification system (Millipore, Bedford, MA, USA) with a resistivity higher than 18 MΩ/cm to prepare all solutions. All the reagents were analytical grade or better.

Scanning electron microscopy (SEM) image was obtained with an S-4800 TEM (Hitachi, Japan). Transmission electron microscopy (TEM) graphic was taken on a Tecnai G2 20 (FEI, USA) operated at 200 kV. Fourier transform infrared (FT-IR) spectra of Fe_3O_4/ZIF-8 and Fe_3O_4 were performed on a Perkin-Elmer Paragon 1000 FTIR spectrometer (Waltham, MA, USA) with the KBr pellet technique ranging 500–4000 cm^{-1}. MALDI-TOF MS analysis was fulfilled using a Bruker Autoflex II mass spectrometer (Bruker Daltonics, Germany) equipped with a nitrogen laser (337 nm wavelength; 3 ns pulse width). The laser power energy was adjusted to 50% of the laser pulse energy. The MALDI-TOF MS measurements were carried out in negative ionization mode, and each mass spectrum was obtained as an average of 500 laser shots.

Synthesis of Fe_3O_4/ZIF-8 nanocrystals. First, Fe_3O_4 microspheres were synthesized in aqueous solution in accordance with a literature method with minor modifications [25]. In brief, 0.68 g of $FeCl_3 \cdot 6H_2O$, 1.2 g of NaAC, and 0.2 g of $Na_3Cit \cdot 2H_2O$ were dissolved in 20 mL of ethylene glycol under magnetic stirring. The obtained homogeneous yellow solution was transferred to a stainless-steel autoclave and then heated to 200°C for 10 h. Second, after the reaction, the product was washed with water and ethanol. Then, 0.175 g of Fe_3O_4 microspheres were dispersed in 10 mL of 50% ethanol solution containing 1 mmol of Zn $(NO_3)_2$ and 0.1 mmol of HCl. Subsequently, 20 mL of 50% ethanol solution containing 10 mmol of HMeIM was added to the previous suspension. The resulting mixture was stirred with ultrasound at room temperature for 10 min. The products were collected with a magnet and washed with ethanol and water. The second process was repeated to increase the thickness of the ZIF-8 shell [26].

Detection of nitro-PAHs with Fe_3O_4/ZIF-8 MNCs as adsorbent and matrix. Stock solutions of nitro-PAHs standards at the concentration of 0.5 µg/µL were prepared by dissolving a proper amount of nitro-PAHs in ACN/DCM (1:1, v/v). Then, 2 mg of Fe_3O_4/ZIF-8 MNCs was suspended in 1 mL of ACN/DCM (1:1, v/v) and sonicated for 5 min. Moreover, 5 µL of the Fe_3O_4/ZIF-8 suspension (2 mg/mL) was added into 100 µL of the nitro-PAH standard solution (0.0004 µg/µL). The mixture was then vortexed for 1 min and saved for enrichment. After 40 min, the Fe_3O_4/ZIF-8 MNCs were segregated by an external magnet and were redispersed in 5 µL of ACN/DCM (1:1, v/v), and 1 µL of the previous mixture was spotted directly onto the MALDI plate. The obtained peak intensity of each nitro-PAH in the enrichment samples was compared with that from the analysis of standard solution at the corresponding level to evaluate the enrichment efficiency. All the abovementioned solutions and suspensions were stored at 4 °C.

Collection and pretreatment of $PM_{2.5}$ samples. The $PM_{2.5}$ sampling site was located on the roof of the Environmental Science and Engineering Research Center in Shanxi University (height ≈25 m), ≈300 m away from a major roadway in the urban site of Taiyuan. The $PM_{2.5}$ sample was gathered using an active sampler (Thermo Andersen, USA) at a flow rate of 1.13 m^3/min. A quartz fiber filter (203×254 mm, Whatman, PMA, GE Healthcare Life Sciences, UK) was used for $PM_{2.5}$ sample collection for 24 h on Nov. 23, 2016.

The $PM_{2.5}$ sample membrane was divided into 1×1 cm size and extracted with two 25 mL of DCM under ultrasonic assistance in a 100 mL breaker. The combined extracts were dried under a stream of nitrogen. Then, the residue was scattered into 100 µL of ACN/DCM (1:1, v/v). Furthermore, 5 µL of the Fe_3O_4/ZIF-8 suspension (2 mg/mL) was put into use for the enrichment of nitro-PAHs in the $PM_{2.5}$ sample extract. The enriched $PM_{2.5}$ samples were analyzed using MALDI-TOF MS with Fe_3O_4/ZIF-8 MNC as the matrix.

Results and discussion. *Characterization of Fe_3O_4/ZIF-8 MNCs.* The synthesized materials were characterized using scanning electron microscopy (SEM) and transmission electron microscopy (TEM). The morphologies of Fe_3O_4/ZIF-8 MNCs were confirmed by SEM and TEM as shown in Fig. 1. The SEM image (Fig. 1a) showed that Fe_3O_4/ZIF-8 MNCs were almost global with an average particle size of 200 nm. Moreover, the TEM image (Fig. 1b) distinctly showed the formation of the ZIF-8 shell of ca. 20 nm in thickness around the Fe_3O_4 core. Both SEM and TEM images indicated numerous ZIF-8 shells on the surface of the Fe_3O_4 core, which showed the successful combination of numerous ZIF-8 nanocrystals on the surface of the Fe_3O_4 core.

The spectrum of Fe_3O_4/ZIF-8 reveals more accessional absorption bands related to the ZIF-8 structure than the spectrum of Fe_3O_4 microspheres (Fig. 2). The absorption bands at 3134 and 2900 cm^{-1} corresponding to the aromatic and aliphatic C–H stretch modes, respectively, are observed in the spectrum of Fe_3O_4/ZIF-8. The stretching vibration band at 1422 cm^{-1} and plane bending vibration in the region of 900–1330 cm^{-1} could be attributed to the imidazole ring. The absorption band at 419 cm^{-1} is assigned to the characteristic Zn–N stretch mode. These data of the FT-IR spectra fully indicated the formation of ZIF-8 shells.

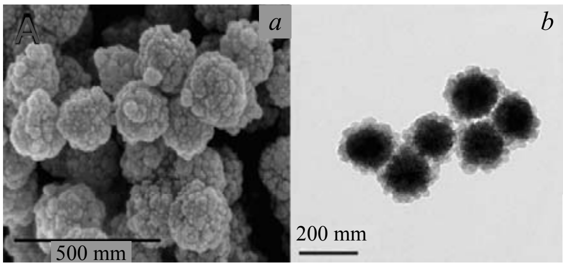

Fig. 1. SEM (a) and TEM (b) images of Fe_3O_4/ZIF-8 MNCs.

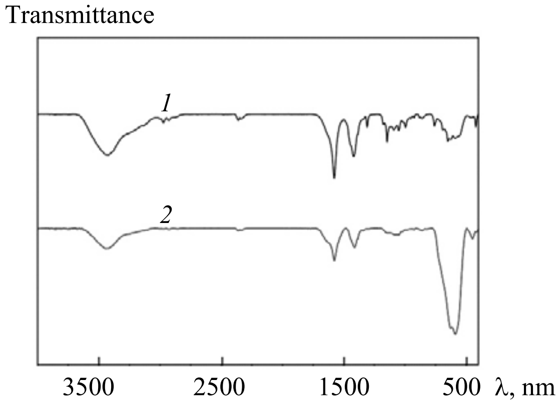

Fig. 2. FT-IR spectra of Fe_3O_4/ZIF-8 (1) MNCs and Fe_3O_4 (2) microspheres.

Optimal experiment conditions. To obtain good enrichment efficiency, common solvents and solvent mixtures were tested, such as DCM, DCM/THF, DCM/acetone, DCM/ACN, ethanol/acetone, and ethanol/THF, in which the volume ratio of solvent mixtures was 1:1. The solvent mixture of DCM/ACN not only provided excellent solubility of four nitro-PAHs but also showed a considerable dispersity of Fe_3O_4/ZIF-8 MNCs. Therefore, the DCM/ACN solvent mixture was selected in following experiment.

Sample preparation steps had important effects on the sensitivity and reproducibility of MALDI-TOF MS. Thus, Fig. 3 displays the MS signals of the 1-NP model sample with three different sample preparation procedures (sample-first, matrix-first, and dried-droplet methods). The signal intensity of 1-NP, which was obtained with the dried-droplet method, was higher (S/N = 235) than that with the previous two methods. The high ionization efficiency can be attributed to the thorough mixing. Thus, the dried-droplet method was selected for further experiments.

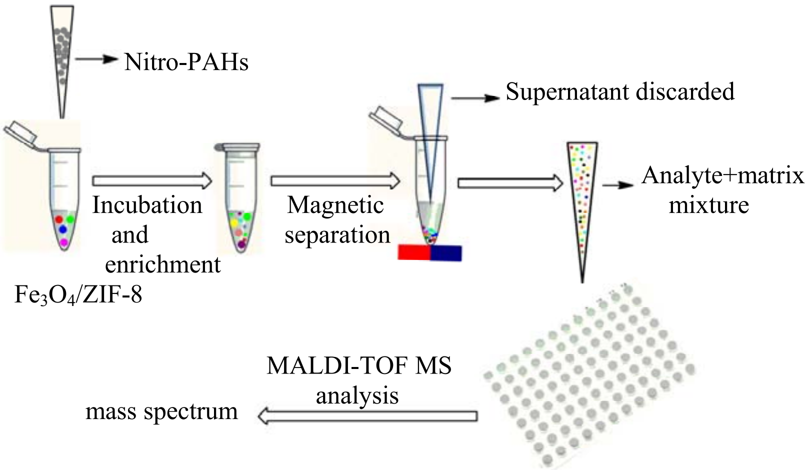

Fig. 3. Schematic representation of operation flow diagram of nitropolycyclic aromatic hydrocarbons.

Application of Fe_3O_4/ZIF-8 MNCs as Matrix in MALDI-TOF MS negative mode. The analysis of four nitro-PAHs was performed to observe whether the nitro-PAHs could be motivated by laser or ionization without any matrix. No peak of nitro-PAHs was detected without using a matrix in MALDI-TOF MS. In view of the special structure of Fe_3O_4/ZIF-8 MNCs, we implement a MALDI-TOF-MS study to investigate the matrix assistance function of the proposed materials using Fe_3O_4/ZIF-8 MNC as the matrix and four nitro-PAHs as molecular models. Considering the structure of nitro-PAHs, the nitro group has more electron affinities than PAHs, and MALDI-TOF MS in negative-ion mode should further easily excite negative ions of nitro-PAHs. Figure 4a–d displays the mass spectra of four nitro-PAHs acquired from the analysis of the standard solution by using Fe_3O_4/ZIF-8 MNC as the matrix in negative desorption/ionization mode. The primary characteristic $[M\text{-}NO]^-$ ion of 1-NP, 6-NC, and 9-NA at m/z = 217.18, 243.11, and 193.18, respectively, predominated their mass spectra. Their minor ion peaks, such as $[M]^-$, $[M+O–H]^-$ at m/z = 247.11, 262.08 for 1-NP, [M]$^-$ at m/z = 223.102 for 9-NA, and [M+O–H]$^-$ at m/z = 288.06 for 6-NC, also were detected (Figs. 4a–c). For 2-NFL, [M-H]$^-$ ion peak at m/z = 210.08 was the base peak, accompanied by a minor peak of [M+O–H]$^-$ (Fig. 4b). 2-NFL may have strong ability of deprotonation, which led to the emergence of the base peak [M–H]$^-$ in the negative-ion mode of MALDI-TOF MS. The appearance of ion peak [M+O–H]$^-$ was due to the ion–molecule reaction, that is, the ions and neutral molecules of the same nitro-PAHs in negative mode.

The traditional matrix, namely, cyano-4-hydroxycinnamic acid (CHCA), was applied for the MALDI-TOF measurement of four nitro-PAHs. Figure 4a′–d′ shows the results. As noted from the mass spectrum, the ion signal of four nitro-PAHs could not be detected and have a strong background interference by using CHCA as the matrix. Thus, Fe_3O_4/ZIF-8 MNC is a more suitable matrix for the MALDI-TOF MS analysis of nitro-PAHs.

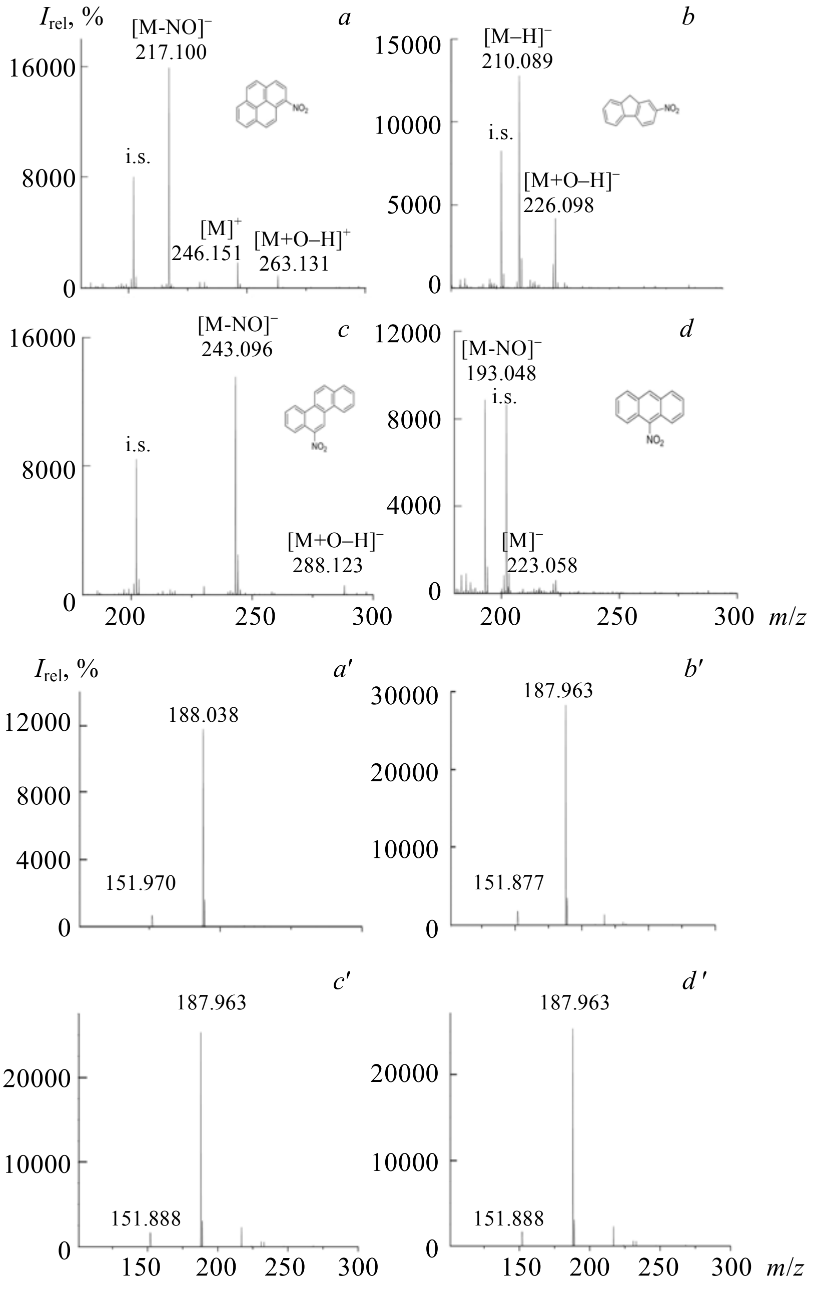

Fig. 4. Mass spectra of 1-nitropyrene (a, a′), 2-nitrofluorene (b, b′), 6-nitrochrysene (c, c′), 9-nitroanthracene (d, d′) using Fe_3O_4/ZIF-8 MNCs in negative-ion mode (a–d) and using CHCA as matrix (a′–d′).

Tables 1 and 2 present the signal reproducibility of four nitro-PAHs obtained using Fe_3O_4/ZIF-8 MNC as the matrix. The relative standard deviations of signal intensity in three replicate analyses for shot-to-shot and sample-to-sample assays were 7.3, 6.8% ($n = 10$) and 16.2, 15.8% ($n = 10$), respectively. The results and the absence of background noise implied that no “sweet spot” question was due to the use of Fe_3O_4/ZIF-8 MNC as the matrix.

The mixture containing four standard nitro-PAHs at 50 pg/µL with the detection of the abovementioned characteristic ions peaks was analyzed using Fe_3O_4/ZIF-8 MNC as the matrix in negative mode (Fig. 5). The exact masses from the detection of the individual standard compound and mixture of the four nitro-PAHs well matched the relevant academic values having an error of less than 15 ppm.

TABLE 1. Linear Equation of Nitro-PHAs Analysis by using MALDI-TOF-MS

Analyte	Linear range, mg/mL	Linear equation, mg/mL	R^2	LOD, ng/µ
1-NP	0.02–1.00	$y = 63.278x - 1.5887$	0.9917	0.47
2-NFL	0.10–2.00	$y = 2.7879x - 0.1447$	0.9984	0.92
6-NC	0.02–2.00	$y = 7.8090x - 0.1047$	0.9909	4.09
9-NA	0.10–2.00	$y = 1.0989x - 0.0299$	0.9991	4.11

TABLE 2. Recovery of the Four Nitro-PHAs

Analyte	Spiked, mg/mL	Measured±SD, mg/mL	Recovery, %
1-NP	0.16	0.145±2.45	90.6
	0.80	0.762±1.27	95.3
2-NFL	0.16	0.124±2.52	77.5
	0.80	0.671±1.89	83.9
6-NC	0.16	0.171±1.44	106.9
	0.80	0.859±1.68	107.4
9-NA	0.16	0.142±1.52	88.7
	0.80	0.639±2.01	79.9

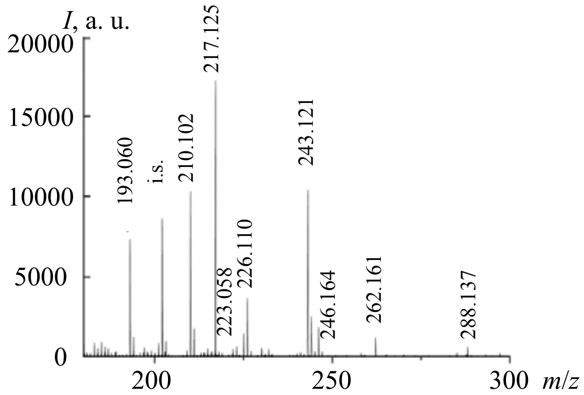

Fig. 5. Mass spectra from the analysis of mixture of nitropolycyclic aromatic hydrocarbons.

Enrichment efficiency of nitro-PAHs with Fe_3O_4/ZIF-8 MNCs as the adsorbents. By using triplicated MOF analysis to execute four nitro-PAHs, the enrichment efficiency and detection limit were studied. The averaged intensities of the primary characteristic ion peak of each nitro-PAH in the extract and of the standard analysis without enrichment were compared to identify the recovery. The recovery of applying 20 µg of Fe_3O_4/ZIF-8 MNCs for the enrichment of 200 µL of the solution containing nitro-PAHs at 50 pg/µL was 73±12% ($n = 10$). In addition, the Fe_3O_4/ZIF-8 MNCs could be repeatedly used with simple recovery. The detection limit of the instrument with an S/N of 3 was evaluated to be 5–8 pg. The measure could be used to analyze the nitro-PAHs at pg/µL levels without the influence of background noise.

Analysis of real environmental samples PM2.5. To validate the usability in practical samples, the proposed method was applied to analyze nitro-PAHs in PM2.5. The extracts of the practical sample were analyzed with Fe_3O_4/ZIF-8 MNc as the matrix in negative mode using MALDI-TOF MS. The average concentration levels of 1-NP, 2-NFL, 6-NC, and 9-NA in the PM2.5 samples were 10.56, 0.90, 11.96, and 10.30 ng/m^3, respectively. The four nitro-PAHs were detected in the extract of practical samples by using the developed method due to their levels in the sample extract of approximately 10–200 pg/μL. Other possible existing nitro-PAHs were not detected due to the lack of standard reference substances. The detected ions of each nitro-PAH involved all their isomers, because the isomers of each corresponding nitro-PAH with the same characteristic ion were not placed through chromatographic separation.

Conclusion. In this work, Fe_3O_4/ZIF-8 MNCs were prepared at room temperature with Fe_3O_4 as the magnetic core, Zn^{2+} ion as the connector, and HMeIM as the linker. The results demonstrated the potential of Fe_3O_4/ZIF-8 MNCs as absorbent and MALDI matrix for the measurement of four nitro-PAHs in negative-ion mode. The Fe_3O_4/ZIF-8 MNCs showed numerous advantages, including interference-free background, high sensitivity, selectivity, and reproducibility in the analysis of four nitro-PAHs. This research proposed a valuable method development for the analysis of nitro-PAHs using Fe_3O_4/ZIF-8 MNCs as enrichment material and matrix for MALDI-TOF MS. This study aimed to detect four nitro-PAHs in the $PM_{2.5}$ sample. Fe_3O_4/ZIF-8 MNC is anticipated to be an alternative matrix to analyze additional environmental pollutants.

Acknowledgment. This work is supported by National Natural Science Foundation of China (21175086), Shanxi Medical University Innovation Fund (01201312), and 331 Early Career Researcher Grant of Shanxi Medical University Medical School Foundation (201417).

REFERENCES

1. M. Gao, P. E. Saide, J. Y. Xin, Y. S. Wang, Z. R. Liu, Y. X. Wang, Z. F. Wang, M. Pagowski, S. K. Guttikunda, G. R. Carmichael, *Environ. Sci. Technol*., **51**, 2178–2185 (2017).
2. Y. Shen, Y. Y. Wu, G. D. Chen, H. J. M. Van Grinsven, X. F. Wang, B. J. Gu, X. M. Lou, *Environ. Pollut*., **224**, 631–637 (2017).
3. Y. M. Guo, H. M. Zeng, R. S. Zheng, S. S. Li, G. Pereira, Q. Y. Liu, W. Q. Chen, R. Huxley, *Sci. Total Environ*., **579**, 1460–1466 (2017).
4. C. B. Song, J. J. He, L. Wu, T. S. Jin, X. Chen, R. P. Li, P. P. Ren, L. Zhang, H. J. Mao, *Environ. Pollut*., **223**, 575–586 (2017).
5. D. M. Agudelo-Castaneda, E. C. Teixeira, I. L. Schneider, S. R. Lara, L. F. O. Silva, *Environ. Pollut*., **224**, 158–170 (2017).
6. X.-Y. Yang, K. Igarashi, N. Tang, J. M. Lin, W. Wang, K. Takayuki, T. Akira, H. Kazuichi, *Mutat. Res. Genet. Toxicol. Environ. Mutagen*., **695**, 29–34 (2010).
7. K. Tanaka, H. Waki, Y. Ido, S. Akita, Y. Yoshida, T. Yohida, *Rapid Commun. Mass Spectrom*., **2**, 151 (1988).
8. P. Hart, E. Wey, T. D. Mchugh, I. Balakrishnan, O. Belgacem, *Microbiol. Methods*, **111**, 1–8 (2015).
9. J. J. A. van Kampen, P. C. Burgers, R. de Groot, R. A. Gruters, T. M. Luider, *Mass Spectrom. Rev*., **30**, 101–120 (2011).
10. R. Arakawa, K. Hideya, *Anal. Sci*., **26**, 1229–1240 (2010).
11. H. Zhang, S. W. Cha, E. S. Yeung, *Anal. Chem*., **79**, 6575–6584 (2007).
12. Q. H. Min, X. X. Zhang, X. Q. Chen, S. Y. Li, J. J. Zhu, *Anal. Chem*., **86**, 9122–9130 (2014).
13. M. H. Lu, Y. Q. Lai, G. N. Chen, Z. W. Cai, *Anal. Chem*., **83**, 3161–3169 (2011).
14. R. N. Ma, M. H. Lu, L. Ding, H. X. Ju, Z. W. Cai, *Chem. Eur. J*., **19**, 102–108 (2013).
15. B. L. Walton, G. F. Verbeck, *Anal. Chem*., **86**, 8114–8120 (2014).
16. Y. F. Huang, H. T. Chang, *Anal. Chem*., **79**, 4852–4859 (2007).
17. J. Wei, J. M. Buriak, G. Siuzdak, *Nature*., **399**, 243–246 (1999).
18. A. Nordstroem, J. V. Apon, W. Uritboonthai, E. P. Sgo, G. Iuzdak, *Anal. Chem*., **78**, 272–278 (2006).
19. C.-K. Chiang, W.-T. Chen, H.-T. Chang, *Chem. Soc. Rev*., **40**, 1269–1281 (2011).
20. Y.-H. Shih, C.-H. Chien, B. Singco, C.-L. Hsu, C.-H. Lin, H.-Y. Huang, *Chem. Commun*., **49**, 4929–4931 (2013).
21. Z. A. Lin, W. Bian, J. N. Zheng, Z. W. Cai, *Chem. Commun*., **51**, 8785–8788 (2015).
22. R. Banerjee, A. Phan, B. Wang, Ca. Knobler, H. Furukawa, M. O’Keeffe, O. M. Yaghi, *Science*, **319**, 939–943 (2008).
23. G. Lu, J. T. Hupp, *J. Am. Chem. Soc*., **132**, 7832–7833 (2010).
24. J. Zheng, C. Cheng, W.-J. Fang, C. Chen, R.-W. Yan, H.-X. Huai, *Cryst. Eng. Commun*., **16**, 3960–3964 (2014).
25. J. N. Zheng, Z. A. Lin, G. Lin, H. H. Yang, L. Zhang, *J. Mater. Chem. B*, **3**, 2185–2191 (2015).
26. Y. C. Pan, Y. Y. Liu, G. F. Zeng, L. Zhao, Z. P. Lai, *Chem. Commun*., **47**, 2071–2073 (2011).